Redesign and Control of a Trolley Propulsion System with a PMSM using FOC

S. Christensen, A. Fenollosa J. Mortensen

Department of Materials and Production, Aalborg University
Fibigerstraede 16, DK-9220 Aalborg East, Denmark
Email: jmor14@student.aau.dk,
Web page: http://www.mechman.mp.aau.dk/

Abstract
This paper continues the work of two previous student projects from Aalborg University, concerning how to improve the existing GEA Mullerup suspended feeding system. In the current solution by GEA, the propulsion system consists of two trolleys mounted with a 165 W DC motor each that drives 4 pulley wheels through a worm gear and two V-belts. The pulley wheels travel along a suspended I-beam. This drive-train is rather inefficient, which is problematic, since the suspended cow feeding trolley runs on batteries [1]. Furthermore, this drive-chain is rather expensive. These factors give reason to redesign the propulsion system of the trolley.
It has been decided to investigate the possibility of using hover-board PMSMs for driving the trolleys. These PMSMs have the capability of being rather efficient and are produced and sold in high numbers, making them fairly cheap.
This paper will focus on redesigning the drive-chain of the trolleys along with implementing and controlling the hover-board PMSM. In order to choose the right drive-chain design, a feasibility study will be conducted to outline the appropriate amount of PMSMs. It is a known feature that worm gears are self-locking. A design constraint is not to use a worm gear as on the existing solution, since it is desirable to implement four-quadrant control, and thus be able to regenerate energy when braking, increasing the energy efficiency of the system.
For implementing a four-quadrant control scheme on the specific motor an inverter will be designed. The field-oriented control (FOC) method will be implemented with the aim of producing high and smooth torque output with low noise.

Keywords: PMSM, FOC, Feasibility Study, Power Consumption & Efficiency

1. Introduction

Unless otherwise specified, this article is based on [2]. GEA Farm Technologies Mullerup A/S is a manufacturer of products for the farming industry. One of their products is an Automatic Feeding System for feeding cows. It is time consuming to feed the cows by hand, so this system helps to save time, and it is also able to deliver the feed in a clean and precise way. The system consists of a container mounted to two battery powered trolleys riding along a suspended I-beam [3]. The container has an empty weight of 1000 [kg], and can be loaded with 2000 [kg] of feed. Each of two the trolleys are driven by a 24 [V] brushed DC motor with a rated efficiency of 68 [%] [4]. The power from the motor is transmitted through a 25:1 worm gear, which drives two V-belts, transmitting the power to the four wheels. The combination of utilising a brushed DC motor and a worm gear is resulting in significant power loses in the power transmission, which creates the interest for investigating other solutions.

One possibility is to make use of a Permanent Magnet Synchronous Machine (PMSM), as it is known for having a high reliability and efficiency, a high peak torque, and a high speed range. Unfortunately, it is also known for having a higher cost, and for needing a more complex controller. Fortunately, the rise in popularity of the so called hoverboards (also known as segboards or self-balancing boards), which utilises two PMSM to drive its two wheels, has driven down the price of spare motors for these products. This creates the idea of investigating other use-cases for these machines.

1.1 System requirements

The aim with the new design is to increase efficiency, and reduce maintenance. This has led to the chosen system requirements, which can split into mechanical, transient and steady-state requirements.

1.1.1 Mechanical requirements

- Fewer parts that require maintenance.
- Must fit the I-beams IPE140 to IPE200.

- The same or improved load capacity as the original design by GEA.
- No slip between driving wheels and I-beam when accelerating.
- The same or an increased efficiency compared to the original design by GEA.

1.1.2 Transient & steady state response requirements

- Maximum linear velocity of trolley: $v_{max} \geq 20\,[\mathrm{m/min}]$
- Deliver corresponding acceleration to the original design.
- Acceleration steady state error: $\dot{\omega}_{ess} \leq 3\,[\%]$
- Velocity overshoot: $\%\mathrm{OS}_{\omega} \leq 1\,[\%]$
- Gain margin: 8 [dB]
- Phase margin: 45 [°]

2. Mechanical design

For the development of a new mechanical design, it is chosen to consider different methods of power transmission. The methods considered are a V-belt, a gearing and a direct drive transmission, which leads to the final choice of the last one. Reasons hereof are the lack of wearing parts, the reduction of power loses in the mechanical design, and the possibility of easily adding more machines, if more torque is needed, since the PMSM is considered a low cost component. The final concept design is shown in Fig. 1.

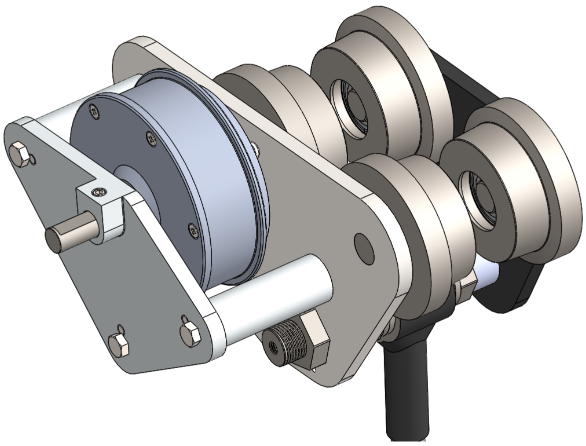

Fig. 1 Final direct drive concept design.

The key components in the new design are:

- A motor holder placing the motor concentrically with respect to the driving wheel
- A driving shaft
- A flexible coupling between the motor and shaft
- A flexible coupling between the wheel and shaft
- A driving wheel that interfaces with the flexible coupling
- A load carrying bearing axle with a hole for a feed through shaft
- A new triangular flange with support for the motor holder and new bearing axle

Without knowledge of load cases that the original solution was designed for, the chosen method for dimensioning the new parts is to make any new load carrying components at least as strong as the original load carrying components. It is chosen not to do any fatigue analysis as the purpose is to construct a working prototype. Analytical calculations for designing against yielding are proposed by [5].

3. Inverter PCB

For the inverter the DRV8353RH three-phase smart gate driver by Texas Instruments was utilized to drive the six CSD19535KCS MOSFETs by Texas Instruments. For supplying signals to the inverter, and for handling feedback signals, a Nucleo STM32F446RE DSP board by STMicroelectronics was used. The main feature of the inverter was to provide a high-power supply for the PMSM. The inverter was designed with the scope of utilising FOC for the PMSM. The design of the inverter was conducted following the recommendations provided with the smart gate driver. A simplified layout of the controller, inverter and PMSM is depicted in fig. 2.

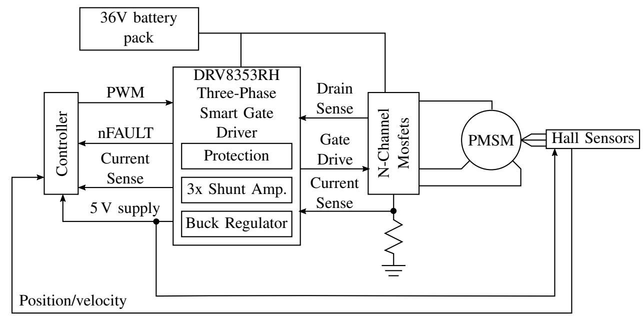

Fig. 2 The simplified layout of the controller, inverter and PMSM.

4. Modelling

This section presents the dynamic model of the PMSM. The machine is modeled in a rotating reference frame, as it simplifies its analysis. Furthermore, the most important assumptions that have been considered will be introduced. Finally, the linear model of the PMSM will be developed, for the future design of the controllers.

4.1 Assumptions for the dynamic model

- **The PMSM is usually a symmetrical machine**. Consequently, the phase resistances, mutual and self inductances, and flux linkages are assumed to be equal, described by R, L_s, L_m and $\hat{\phi}_{pm}$.
- **Permanent magnets are surface mounted and they have no saliency**. Thus, the reluctance paths are the same and the inductances on the d and q-axis can be assumed to be equal ($L_q = L_d$).
- **No saturation in the magnetic circuits is assumed.**
- **Armature reaction effect on the flux linkage and inductance in the d-axis is neglected**.
- **It is assumed that the generated back EMF is purely sinusoidal**.
- **Effects of temperature are not modeled**. The resistance of the copper windings can increase by a $40\,\%$ when the change in temperature is about $100\,°\mathrm{C}$. Consequently, the designed controllers consider this phenomena.

4.2 Dynamic model of the PMSM

The mathematical model describing the Surface Mounted PMSM is presented below. It can be divided into two systems: The electrical and the mechanical system. The electrical system is based on non-linear differential voltage equations, whereas the mechanical system is based on Newton's Second Law of Inertia.

4.2.1 Electrical system

The PMSM is modelled as a three phase star connected system where the three phases are symmetrically distributed 120° from each other, as depicted in fig. 3.

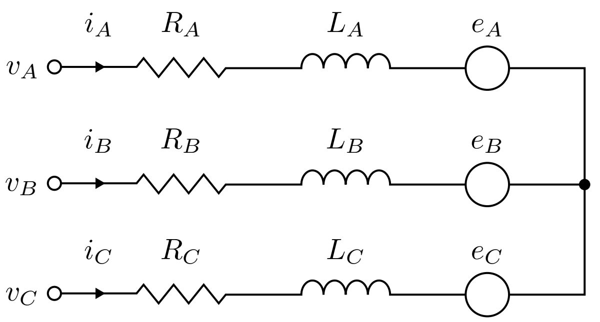

Fig. 3 Three-phase star connection of the PMSM

The voltage equation (eq. 1) consists of Ohm's law and Faraday's induced voltage law; it is the sum of the resistive voltage drops and the sum of all flux linkages in the machine. The flux linkage in each phase can be divided into three components: The first one is the flux contribution from the phase itself, which introduces the concept of self-inductance. The second one is the flux that is linking with the other phases, which introduces the concept of mutual-inductance. The last one is the flux linking with the permanent magnet, which is usually referred as back-EMF.

$$\begin{bmatrix} v_A \\ v_B \\ v_C \end{bmatrix} = \begin{bmatrix} R & 0 & 0 \\ 0 & R & 0 \\ 0 & 0 & R \end{bmatrix} \begin{bmatrix} i_A \\ i_B \\ i_C \end{bmatrix} + \begin{bmatrix} L_s & L_m & L_m \\ L_m & L_s & L_m \\ L_m & L_m & L_s \end{bmatrix} \frac{\mathrm{d}}{\mathrm{d}t} \begin{bmatrix} i_A \\ i_B \\ i_C \end{bmatrix} + \hat{\phi}_{pm} \frac{\mathrm{d}}{\mathrm{d}t} \begin{bmatrix} \cos\theta_e \\ \cos\left(\theta_e - \frac{2\pi}{3}\right) \\ \cos\left(\theta_e - \frac{4\pi}{3}\right) \end{bmatrix} \tag{1}$$

Where:
R: Phase resistance.
L_s: Self-inductance.
L_m: Mutual-inductance.
$\hat{\phi}_{pm}$: Amplitude of the flux linkage of the permanent magnet.
θ_e: Angular position of the rotor.

In order to simplify the system, Kirchoff Current Law can be introduced. As the machine is modelled with an star connection, the previous law states that the sum of the currents in the star point is zero:

$$i_A + i_B + i_C = 0 \tag{2}$$

Consequently, Equation 1 becomes:

$$\begin{bmatrix} v_A \\ v_B \\ v_C \end{bmatrix} = \begin{bmatrix} R & 0 & 0 \\ 0 & R & 0 \\ 0 & 0 & R \end{bmatrix} \begin{bmatrix} i_A \\ i_B \\ i_C \end{bmatrix} + \begin{bmatrix} L_s - L_m & 0 & 0 \\ 0 & L_s - L_m & 0 \\ 0 & 0 & L_s - L_m \end{bmatrix} \frac{\mathrm{d}}{\mathrm{d}t} \begin{bmatrix} i_A \\ i_B \\ i_C \end{bmatrix} + \hat{\phi}_{pm} \frac{\mathrm{d}}{\mathrm{d}t} \begin{bmatrix} \cos\theta_e \\ \cos\left(\theta_e - \frac{2\pi}{3}\right) \\ \cos\left(\theta_e - \frac{4\pi}{3}\right) \end{bmatrix} \tag{3}$$

This is the voltage equation defined in the ABC frame. However, as it was mentioned before, it is easier to model the machine in a rotating reference frame. Thus, coordinate transformations will be used. First, the three phases expressed in the ABC coordinates will be transformed into a two-coordinate stationary reference frame, defined by the $\alpha\beta$ axis. This transformation is called **Forward Clarke transformation**. Then, the two-coordinate reference system will be transformed into a rotating reference frame defined in the dq axis. This transformation is called **Forward Park**

transformation. The equations used for these reference frame transformations are presented below.

Forward Clarke Transformation
As there is a redundant phase in a three-phase machine, the system can be simplified by transforming from the ABC to the $\alpha\beta$ stationary reference frame. The result is two orthogonal vectors, as it can be seen in fig. **??**.

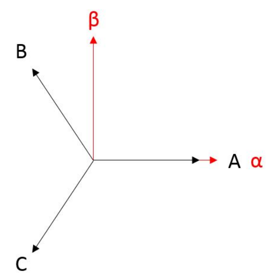

Fig. 4 alpha beta coordinates

The equations of the transformation are:

$$v_{\alpha\beta} = \frac{2}{3}\begin{bmatrix} 1 & -\frac{1}{2} & -\frac{1}{2} \\ 0 & \frac{\sqrt{3}}{2} & -\frac{\sqrt{3}}{2} \end{bmatrix}\begin{bmatrix} v_A \\ v_B \\ v_C \end{bmatrix} \tag{4}$$

Forward Park Transformation
The $\alpha\beta$ stationary reference frame can be transformed into a dq rotating reference frame, where it is easier to model and control the machine, by using this transformation. The result is two rotating and orthogonal vectors, where the d axis is chosen to be orientated in the direction of the rotor flux, in order to obtain maximum torque.

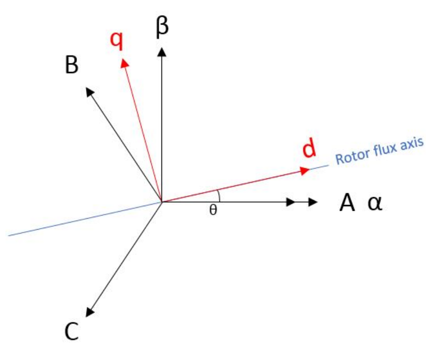

Fig. 5 d q coordinates

The equations of the transformation are:

$$v_{dq} = \begin{bmatrix} \cos\theta_e & \sin\theta_e \\ -\sin\theta_e & \cos\theta_e \end{bmatrix}\begin{bmatrix} v_\alpha \\ v_\beta \end{bmatrix} \tag{5}$$

Where θ_e is the angular position of the rotor.

If these transformations are applied to eq. 3, it becomes:

$$v_d = Ri_d + L\frac{di_d}{dt} - \omega_e L i_q \tag{6}$$

$$v_q = Ri_q + L\frac{di_q}{dt} + \omega_e(Li_d + \hat{\phi}_{pm}) \tag{7}$$

Which are the voltage equations defined in the rotating reference frame.

4.2.2 *Mechanical system*

The mechanical system is described by Newton's Second Law of Inertia (eq. 8).

$$J\frac{d\omega_m}{dt} = \tau_e - B\omega_m - \tau_{df}\, sign(\omega_m) \tag{8}$$

Where:
J: Inertia of the system.
ω_m: Mechanical angular speed.
τ_e: Electro-mechanical torque.
B: Viscous friction.
τ_{df}: Coulomb friction.

It can be seen that there is no load torque component; this is because there is no external load connected to the system.

4.2.3 *Electro-mechanical torque*

The connection between the electrical and mechanical systems is based on the electro-mechanical torque. This can be derived from the power approach.

The instantaneous power applied to the PMSM is:

$$\begin{aligned} P_{in_{PMSM}} &= \frac{3}{2}(v_d i_d + v_q i_q) \\ &= \frac{3}{2}\left[\left(R(i_d^2+i_q^2)\right)+L\left(i_d\frac{di_d}{dt}+i_q\frac{di_q}{dt}\right)+\left(i_q\omega_e\hat{\phi}_{pm}\right)\right] \\ &= P_{cu} + P_b + P_{em} \end{aligned} \tag{9}$$

Where:
P_{cu}: Power due to the copper loss.
P_b: Power due to the magnetic field change of energy.
P_{em}: Electro-mechanical power.

The electro-mechanical power can also be defined in terms of torque and angular velocity, as seen in Equation 10.

$$P_{em} = \tau_e\omega_m = \tau_e\frac{1}{p}\omega_e \tag{10}$$

Where:
ω_e: Electrical angular velocity.
p: Pole pairs.

If eq. 9 and eq. 10 are combined, it its found an expression that links the electro-mechanical system:

$$\tau_e = \frac{3p}{2} i_q \hat{\phi}_{pm} \tag{11}$$

This is for the case of one machine. Thus, Equation 11 in a general form it would be:

$$\tau_e = \frac{3p}{2} i_q \hat{\phi}_{pm} n_m \tag{12}$$

Where n_m is the number of machines.

4.2.4 Model parameters

In this section all parameters that are used to model the PMSM are shown. They are separated into certain and uncertain parameters, as some of them were not measured. Regarding the number of machines (n_m), it is considered as a parameter, but it is not included as its value is one of the conclusions of the project.

Tab. I The parameters that are regarded certain.

Parameter	Value	Units	Description
p	15	[-]	Pole pairs
R	266.6	[mΩ]	Resistance of the winding
r_{wheel}	40	[mm]	Wheel radius
n_r	8	[-]	No. of wheels
M_{cart}	1000	[kg]	Cart mass
M_{feed}	2000	[kg]	Total feed mass
J_{cart_f}	4.8	[kg/m^2]	Inertia of the cart at full load
J_m	8.1×10^{-4}	[kg/m^2]	Motor inertia
J_w	1.1×10^{-3}	[kg/m^2]	Wheel inertia
J	$0.00081 n_m + 4.8088$	[kg/m^2]	Inertia of the whole system

Tab. II The parameters that are not regarded certain.

Parameter	Value	Units	Description
B	0.5	[Nm]	Viscous friction
τ_{df}	0.1	[Nms/rad]	Coulomb friction
L	6.4	[mH]	Inductance of the winding
$\hat{\phi}_{pm}$	21.6	[mWb]	Flux linkage amplitude of the permanent magnet

4.3 Linear system

In order to design controllers it is convenient to linearise the non-linear systems presented above. Thus, in this section both the electrical and the mechanical systems are linearised.

4.3.1 Linearisation of the electrical system

The non-linear voltage equations defined in eq. 6 and 7 describe a coupled system, being the coupling terms:

$$v_{d_{coupling}} = -\omega_e L i_q \tag{13}$$

$$v_{q_{coupling}} = \omega_e (L i_d + \hat{\phi}_{pm}) \tag{14}$$

In order to obtain a linear model both coupling terms are neglected, which ends with having two SISO systems that are linear and independent from each other.

$$v_d = R i_d + L \frac{di_d}{dt} \tag{15}$$

$$v_q = R i_q + L \frac{di_q}{dt} \tag{16}$$

The transfer function of the electrical system is the following:

$$G_{el}(s) = \frac{i(s)\ [\mathrm{A}]}{v(s)\ [\mathrm{V}]} = \frac{1}{Ls + R} \tag{17}$$

As it can be seen, it is a first order system.

4.3.2 Linearisation of the mechanical system

The linearisation of the mechanical system removes the Coulomb friction for being a constant. The transfer function of the mechanical system is:

$$G_{mech}(s) = \frac{\omega_m(s)\ [\mathrm{rad/s}]}{i_q(s)\ [\mathrm{A}]} = \frac{3p\hat{\phi}_{pm} n_m}{2} \frac{1}{Js + B} \tag{18}$$

Which is again a first order system.

5. Control

In this section the structure and steps of Field Oriented Control are explained and controllers for the linear systems are developed. Furthermore, for development of the outer velocity loop, the basic idea is that the current requirement is limited by the slope of the velocity reference curve and that the acceleration steady state error is limited by the gain of the velocity controller. In order to limit the current, the velocity reference curve will be developed. As it is a system requirement, the slope will be based on the acceleration of the original design.

5.1 Reference Curve

Based on an estimated maximum acceleration and velocity capability, eq. 19 and 20, of the original design by GEA a trapezoidal velocity reference curve is established, depicted in fig. 6.

$$v_{lin} \approx 20\,[\mathrm{m/min}] = 1/3\,[\mathrm{m/s}] \tag{19}$$

$$\dot{v}_{lin} \approx 300\,[\mathrm{m/min^2}] = 1/12\,[\mathrm{m/s^2}] \tag{20}$$

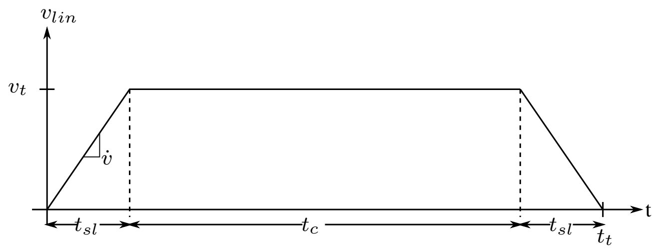

Fig. 6 Trapezoidal reference velocity curve.

Hence, this acceleration capability and maximum speed is applied as a requirement for the final design.

5.2 Field Oriented Control

The way torque is produced in the PMSM is by the interaction between the stator and the rotor magnetic fields. The net magnetic field in the stator is produced by the sum of the individual magnetic fields from the stator windings, when current is flowing through them. The magnetic field in the rotor is produced by the permanent magnets. When these two vectors are orthogonal the produced torque is maximum. Consequently, a good control method will ensure that the torque is maximum at any time.

The control structure implemented in this project is called Field Oriented Control (FOC), also referred to as Vector Control, and it is based on this previous mentioned principle. Basically, the controllers know the orientation of the magnetic field and position of the rotor and generate reference voltages that are supplied to the PMSM in order to generate a net magnetic field vector in the stator that is orthogonal with the one produced by the rotor. Consequently, the controllers ensure that at any instant of time the torque produced is maximum. The process of Field Oriented Control can be described in the following steps:

1) Measurement of the phase currents and estimation of the angle of the rotor.
2) Comparison between the measured current with the desired one and generation of the error signal.
3) Generation of the reference voltage in the controllers from the error signal.
4) Modulation of the reference voltage to be applied on the phase terminals of the machine.

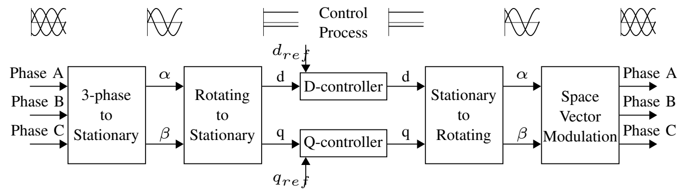

Fig. 8 Overview of the process of Field Oriented Control

One important characteristic of FOC is that signals are controlled in a rotating reference frame. In the stationary reference frame the signals are AC, and tracking a time-variant target from a stationary reference frame is not easy. Consequently, it is defined a new coordinate system that is rotating synchronously with the rotor, based on the direct (d) and quadrature (q) axis, where this last one is aligned with the rotor. In this reference frame, the signals result in DC quantities, which are easier to control. The way this transformations are done is by using Forward Clarke and Park transformations.

However, the voltages applied to the machine terminals need to be in the stationary reference frame defined in the ABC axis. Consequently, Backward Clarke is implemented in order to obtain the voltages defined in the $\alpha\beta$ axes, which will then be modulated via Space Vector Pulse Width Modulation and by means of six MOSFETs it will be possible to emulate the AC signals.

5.3 Controllers design

In this subsection the controllers for the linear electro-mechanical systems are developed. The control structure is based on a cascade scheme, which consists of an inner current and an outer speed loop, as it can be seen in Figure 7.

5.3.1 Current controllers

The controller design is the same for both voltage equations v_q and v_d. The controllers used are PI controllers, where the gains are chosen by using the method of Zero-Pole Cancellation. When the poles of the system are placed on the LHP, this allows to cancel the effect of the pole by introducing a zero on the top of it. The proportional gain (K_p) is found by evaluating the system at its bandwidth:

$$K_p = \frac{1}{|G_{elec}(j \cdot BW_{G_{el}})|} = 0.5325 \tag{21}$$

As the pole of the system is located at $s = -\frac{R}{L}$. Then the integral gain can be found as:

$$s = -\frac{K_i}{K_p} = -\frac{R}{L} \tag{22}$$

$$K_I = \frac{R}{L}K_p = 0.2836 \tag{23}$$

As the pole introduced by the PI is placed at $s = 0$ and as the pole of the system is cancelled by the zero of the controller, then the system can be regarded as a free integrator.

5.3.2 Speed controllers

The controller used is again a PI controller. The procedure for calculating the gains is the same as before. Thus, the gains of the controller are expressed as:

$$K_p = \frac{1}{|G_{mec}(j \cdot BW_{G_{mec}})|} \tag{24}$$

$$K_i = K_p \cdot \frac{B}{J(n_m)} \tag{25}$$

The number of PMSMs is not known yet and is therefore regarded as a variable. Furthermore, the close-loop system is defined as:

$$G_{mech.cl}(s) = \frac{1}{1 + D_{mec} \cdot G_{mec}} \tag{26}$$

As seen, this is a type 1 system. As the applied reference is a ramp, the steady state error will not be zero. In order to satisfy the system requirements, it is needed to reduce the steady state error, which is defined by K_v:

$$K_v = \lim_{s \to 0} sD_{mec}(s)G_{mec}(s) \tag{27}$$

Then, the gain the controllers are multiplied with in order to reduce the steady state error is:

$$K_{ss} = \frac{K_v^{-1}}{\dot{\omega}_{ess}} \tag{28}$$

Where,
$\dot{\omega}_{ess}$: maximum allowable steady state error.

5.4 Feasibility Study

By implementing the described controller development method for the velocity controller as an algorithm as function of the number of PMSMs, a sweep from 1 to 8 PMSMs is performed. From the developed power equations, the efficiency of the system is introduced by eq. 29.

$$\begin{aligned} \eta &= \frac{P_{em}}{P_{in}} = \frac{\tau \cdot \omega_{mech}}{P_{cu} + P_b + \tau \cdot \omega_{mech}} \\ &= \frac{E_{em}}{E_{cu} + E_{em}} \end{aligned} \tag{29}$$

Here, the E_{em} is the output energy and E_{cu} is the copper energy loss. Based on the linearised dynamic models, the torque, mechanical velocity and quadrature axis current is obtained over the course of the reference curve and the energies E_{em} and E_{cu} are obtained by eq. 30 and 31.

$$E_{em} = n_m \cdot \int_0^{2 \cdot t_{sl} + t_c} \tau \cdot \omega_{mech} dt \tag{30}$$

$$E_{cu} = n_m \cdot \int_0^{2 \cdot t_{sl} + t_c} \frac{3}{2} \cdot I_q^2 \cdot R_w dt \tag{31}$$

The sweep of 1 to 8 PMSMs then yield the results of tab. III.

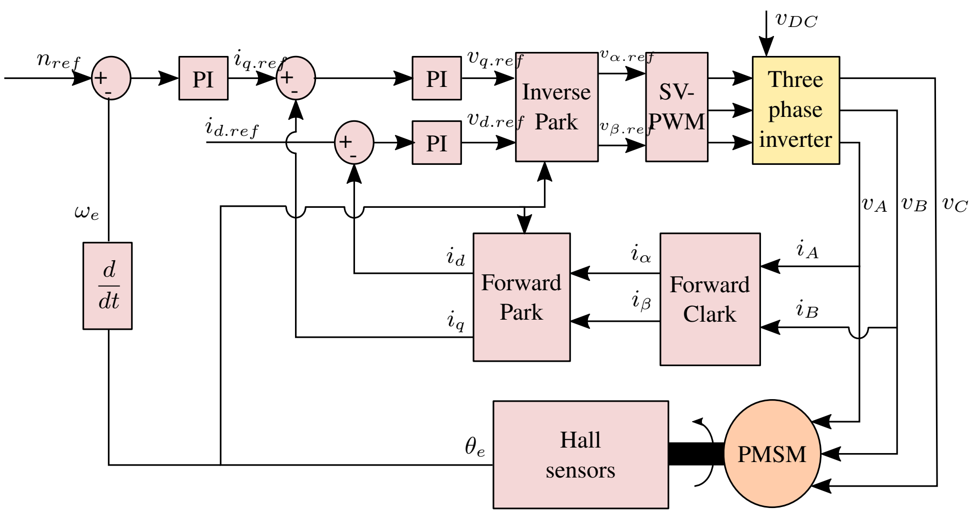

Fig. 7 Cascade control scheme of Field Oriented Control

Tab. III The energy due to copper losses, E_{cu}, the output energy, E_{em}, and the derived efficiency, η, based on the amount of motors, n_m, for the defined velocity reference curve.

n_m	E_{cu}[J]	E_{em}[J]	η[%]
1	2017.47	786.91	28.06
2	1008.90	786.93	43.82
3	672.71	786.96	53.91
4	504.63	786.98	60.93
5	403.78	787	66.09
6	336.54	787.02	70.05
7	288.52	787.04	73.17
8	252.51	787.06	75.71

Based on this, it is decided to use 4 PMSMs for the final design, yielding the PI controllers of eq. 32 and 33 as well as the performance figures of tab. IV.

$$D_{vel} = \frac{5.501s + 0.5716}{s} \tag{32}$$

$$D_{el} = \frac{0.5326s + 22.07}{s} \tag{33}$$

Tab. IV Performance figures with respect to the defined requirements.
$\surd$ = Requirement met. $\times$ = Requirement not met.

Transfer function (equation)	32	33
Acceleration steady state error	3 % $\surd$	
Velocity overshoot	0 % $\surd$	
Gain margin	∞ $\surd$	∞ $\surd$
Phase margin	90 [°] $\surd$	90 [°] $\surd$

6. Implementation

For implementing the FOC through the use of the designed inverter, the PWM generation method Space Vector PWM (SV-PWM) is utilized. SV-PWM is based on describing eight possible inverter gate combinations by six basic vectors and two zero vectors. The six basic vectors are depicted in fig. 9. Within each sector, the voltage reference vector angle and magnitude is used to define the duty cycle of each of the neighboring basic vectors.

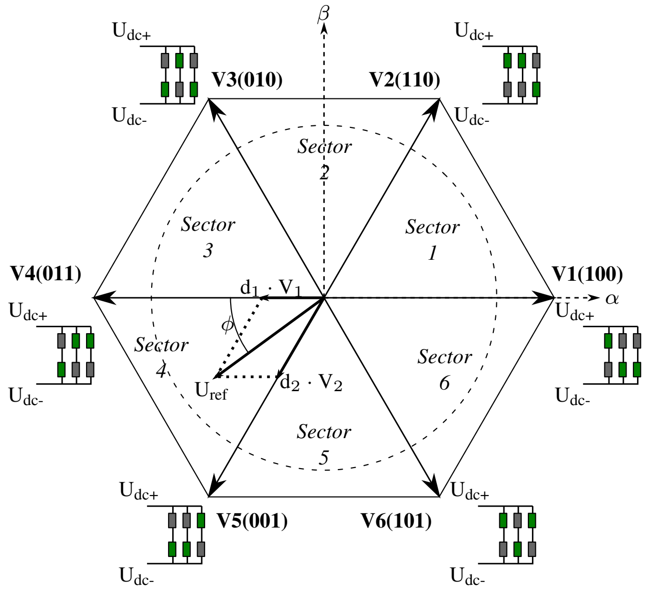

Fig. 9 The six sectors of SV-PWM with an illustration of the duty cycle of each of the neighboring basic vectors, based on the reference voltage vector, U_{ref}.

The result of this modulation technique is a three phase sinusoidal signal with an addition of a triangular signal with a frequency corresponding to the third harmonic of the fundamental frequency. The advantage of this addition is that the output voltage can be increased by 14 %, compared to a three phase sinusoidal signal.

Usually dead-time insertion into the PWM signal is necessary, but this is not the case for the designed inverter since it has automatic dead-time insertion, both taking care of not short-circuiting the inverter, but also for charging the bootstrap capacitor for driving the high gates.

Based on the hall sensor feedback, for every rising or falling edge, the rotor position is known. A backwards finite difference approximation is used to estimate the velocity at each edge detection. In order to increase the resolution of the position the last known velocity is used to extrapolate the last known position and obtain an assumed position.

7. Results

The inverter did not function in due time. Therefore, the controllers are only evaluated by simulation. For the non-linear system, the SV-PWM is implemented, while the hall sensor feedback is left for future work.

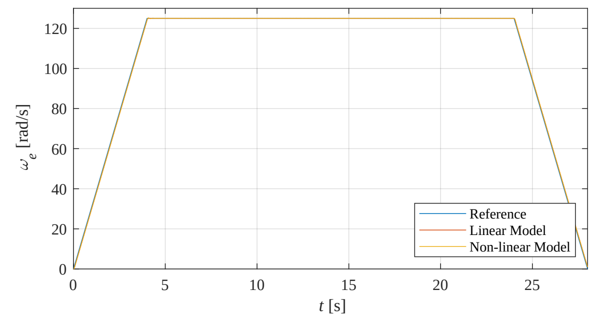

Fig. 10 Simulated validation of the developed controllers against the linear and non-linear systems.

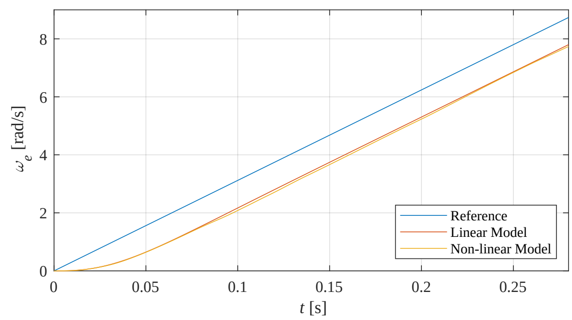

Fig. 11 Simulated validation of the developed controllers against the linear and non-linear systems. The linear and non-linear models display virtually identical responses.

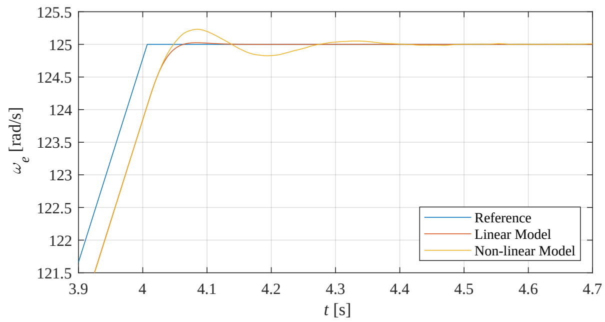

Fig. 12 Simulated validation of the developed controllers against the linear and non-linear systems. A slight overshoot is visible for the non-linear model, but is approximately 0.002 %, hence deemed negligible.

Based on these simulations, the controllers are verified, though clearly lack practical implementation to validate against experimental setup.

8. Conclusion

Based on the simulations and evaluation of the system requirements, it is deemed that the designed trolley and control system for the full load feeding system comply with all set requirement, though not validated experimentally.

Acknowledgement

The authors of this work gratefully acknowledge Grundfos for sponsoring the 7th MechMan symposium.

References

[1] E. Falcon, S. R. Sørensen, and S. Pellegrino, "Implementation of a permanent magnet synchronous motor drive system in a suspended trolley machine," tech. rep., Aalborg University, 2018. 8th semester project at Electro-Mechanical System Design, AAU.

[2] S. B. Christensen, A. F. Hontecillas, and J. Mortensen, "Redesign and control of a trolley propulsion system with a pmsm using foc," tech. rep., Aalborg University, 2019. 8th semester project at Electro-Mechanical System Design, AAU.

[3] "GEA website." https://www.gea.com/, 2019. [Online; accessed 2019-05-08].

[4] TEM Electric Motors, DC Motor PML Datasheet, 2019.

[5] R. L. Norton, Machine Design: An Integrated Approach. No. ISBN: 978-0-13-335671-7 in 5th edition, Pearson, 2014.